Revealing temperature fields of thermal models basing on multichannel measurement and simulation *

Zweig, Wong[1†]
1 Zhongshan School of Medicine, Sun Yat-sen University, Guangzhou 510275, China

Abstract: Revealing temperature field distribution and its evolution along with time in components under certain thermal stress is a critical issue. Taking advantages of computer-based multichannel virtual instruments and Multiphysics Simulation software, we aimed to investigate and reveal the general characteristics of temperature fields of typical thermal conduction models. In this research, we constructed the resistor thermal model and the plate thermal model and conducted real-world temperature measurement and simulation experiments for both models based on LabVIEW and COMSOL, respectively. Measurements of real-world temperature fields and simulation output were compared. The results show that for the resistor heating model, as the current starts to flow through the resistor, the surface temperature began to increase. After a rapid climb of the temperature, the thermal system gradually reached an equilibrium, and the temperature finally become stable. If the current was removed, the temperature began to drop and finally reached room temperature. What's more, comparing the equilibrium temperatures of the four resistors, we found that as the resistance value increased, the equilibrium temperature increased, which is in our expectations. We also found that the equilibrium temperature was directly proportional to the resist value. As for the plate thermal model, we found that after a short period of non-linear increasing, the surface temperature finally reached a "linear zone", in which the temperature was directly proportional to the heating time. When comparing real-world models and simulation models, we found that although the measurement values were not exactly consistent due to the lack of the necessary and pivotal exact values of material properties and geometric dimensions, the tendencies and general patterns of temperature changes are identical, which proves the effectiveness of these techniques in studying thermal conducting models with very complex boundary conditions. In conclusion, in this research we conducted real-world temperature measurement basing on LabVIEW, and simulation experiments basing on COMSOL for both the resistor thermal model and the plate thermal model, and revealed the characteristics of temperature fields of these models and their evolution over time. Our work proves the effectiveness of computer-based multichannel virtual instruments and Multiphysics Simulation software in studying thermal conducting models with very complex boundary conditions, and may provide new insights for the general characteristics of temperature fields of these typical thermal conducting systems.

Keywords: Temperature field, Virtual instruments, Multiphysics Simulation software, thermal conduction models, multichannel measurement, simulation

1 Introduction

Revealing and controlling the distribution of temperature fields in components under certain thermal stress are critical technical issues in industrial design. Traditionally, temperature sensors are embedded in certain situs of the component, and changes of temperature over time are measured and obtained separately. This method, exact though it is, has lots of limitations. First, the sensors work separately, making it difficult to synchronize the measurements. Second, due to the limitation of number of sensors, it is difficult to obtain the full picture of real-time temperature distribution.

With the rapid development of temperature measurement techniques, computer-based multichannel virtual instruments have been developed and widely applied in studying thermal conduction models, which integrate multichannel temperature sensors and enable multichannel synchronous measurements. One representative platform is LabVIEW (Laboratory Virtual Instrument Engineering Workbench) developed by NI, which is highly modular and integrative, allowing convenient virtual instrument design and multichannel synchronous signal acquisition. What's more, Multiphysics Simulation software such as COMSOL, which is able to solve partial differential equations under very complex boundary conditions using finite element method, allow researchers to obtain the full picture of simulated real-time temperature distribution under certain conditions easily and conveniently. The theoretical basis of this computational framework is solid, and what users only need to do is constructing a proper simulated model and setting up necessary parameters, and the model will return a wealth of information about the system including the simulated field distribution and its revolution along with time. These new techniques effectively address the problems of traditional methods.

In this research, we conducted real-world temperature measurement basing on the LabVIEW platform, and simulation experiments basing on COMSOL for

*Supported and taught by Luyoutang, School of Physics, Sun Yat-sen University
†Corresponding author. ID: 20980066 Email: huangzw29@mail2.sysu.edu.cn

both the resistor thermal model and the plate thermal model, and revealed the characteristics of temperature fields of these models and their evolution over time.

2 Experimental principles and method

2.1 Experimental principle[1]

2.1.1 The ideal resistor thermal model

The ideal resistor thermal model is illustrated as Fig. 1a. Take the column coordinate system (r, θ, z) and assume that the resistor is an ideal homogeneous cylinder (radius: a, height: b, volume: V, density: ρ, specific heat: c, and resistance: R) with current I uniformly distributed along the z-direction, the heat flux q satisfies Fourier's law:

$$\boldsymbol{q} = -k\nabla u \tag{1}$$

where k is the thermal conductivity and $u = u(r, z, t)$ is the temperature field of the resistor over time. Then u satisfies the following fixed solution problem:

$$\begin{cases} \dfrac{\partial u}{\partial t} - \kappa\nabla^2 u = \dfrac{I^2 R}{c\rho V}, \quad \kappa = \dfrac{k}{c\rho} \\ u_{|t=0} = u_0 \\ \dfrac{\partial u}{\partial r}_{|r=a} = -\dfrac{Q_r}{2\pi abk}, \quad u_{|r=0}\ finite \\ \dfrac{\partial u}{\partial z}_{|z=0} = \dfrac{Q_1}{\pi a^2 k}, \quad \dfrac{\partial u}{\partial z}_{|z=b} = -\dfrac{Q_2}{\pi a^2 k} \end{cases} \tag{2}$$

where $u0$ is the initial temperature field, and $Q1, Q2, Qr$ represents the amount of heat flowing through the bottom, top and side face per unit time, respectively.

The analytical solution of this fixed solution problem is:

$$\begin{aligned} u =& (\frac{I^2 R}{c\rho V} - \kappa\frac{Q_1 + Q_2 + Q_r}{\pi k a^2 b})t \\ & - \kappa\frac{Q_r}{4\pi k a^2 b}r^2 + \frac{Q_1}{\pi k a^2}z - \frac{Q_1 + Q_2}{2\pi k a^2 b}z^2 + u_0 \\ & + \sum_{i=1}^{\infty} \frac{1}{\lambda_i^2 a^2 J_0^2(\lambda_i a)} \frac{Q_r}{\pi k b} J_0(\lambda_i a) J_0(\lambda_i r) e^{-\kappa\lambda_i^2 t} \\ & + \sum_{i=1}^{\infty} \frac{2b}{n^2\pi^3 k a^2}[Q_1 + (-1)^n Q_2] cos\frac{n\pi}{b} z e^{-\kappa(\frac{n\pi}{b})^2 t} \end{aligned} \tag{3}$$

where $Jm(x)$ is M-order Bessel Function, $Jm'(x) = \frac{d}{dx}Jm(x)$, λ_i is ith non-negative root of the equation $J_0(\lambda a) = 0$, $i = 0, 1, 2, 3, ...$ satisfying $\lambda_0 = 0 < \lambda_1 < \lambda_2 < \Lambda$.

This model, however, is far from the real-world situation, where the side face of the resistor will exchange heat with surroundings following Newton's law of cooling:

$$\boldsymbol{q} \cdot \boldsymbol{e_r}_{|r=a} = g(u_{|r=a} - u_{ext}) \tag{4}$$

where u_{ext} is the surrounding temperature, g is the heat exchange coefficient. Take $h = \frac{g}{k}$, the side face satisfies the third boundary condition:

$$(\frac{\partial u}{\partial r} + hu)_{|r=a} = hu_{ext} \tag{5}$$

Too complex the model is, it's difficult to give an analytical solution using variable separation approach, let alone the resistor is actually a shell with ceramic filling inside rather than a solid cylinder (Fig. 1b). With the aid of COMSOL, it is possible to give a numerical solution based on the finite element method.

2.1.2 The ideal plate thermal model

The ideal plate thermal model is illustrated as Fig. 2. Consider an infinite flat-plate poor thermal conductor (thickness: $2R$, density: ρ, specific heat: c, thermal conductivity: λ) with a uniform heat flow q_c pointing to the center surface applied simultaneously on both sides, the temperature $t(x, \tau)$ satisfies the following fixed solution problem:

$$\begin{cases} \dfrac{\partial t(x,\tau)}{\partial \tau} - \dfrac{a\partial^2 t(x,\tau)}{\partial x^2} = 0 \\ \dfrac{\partial t(R,\tau)}{\partial x} = \dfrac{q_c}{\lambda}, \quad \dfrac{\partial t(0,\tau)}{\partial x} = 0 \\ t(x, 0) = t_0 \end{cases} \tag{6}$$

where t_0 is the initial temperature, $a = \frac{\lambda}{\rho c}$, $q_c = c\rho R\frac{\partial t}{\partial \tau}$.

If the heating time τ satisfies $\frac{a\tau}{R^2} > 0.5$, the analytical solution of this fixed solution problem can be simplified as

$$t(x, \tau) = t_0 + \frac{q_c}{\lambda}\left(\frac{a}{R}\tau + \frac{1}{2R}x^2 - \frac{R}{6}\right) \tag{7}$$

The temperature of the center $(x = 0)$ and surface $(x = R)$ face of the sample are:

$$\begin{cases} t(0, \tau) = t_0 + \dfrac{q_c}{\lambda}\left(\dfrac{a}{R}\tau - \dfrac{R}{6}\right) \\ t(R, \tau) = t_0 + \dfrac{q_c}{\lambda}\left(\dfrac{a}{R}\tau + \dfrac{R}{3}\right) \end{cases} \tag{8}$$

And their difference and the heating rate are:

$$\Delta t = \frac{q_c R}{2\lambda} \tag{9}$$

$$v = \frac{aq_c}{\lambda R} \tag{10}$$

Obviously, at this stage, the temperature of the sample increase linearly and Δt remain constant, which is called the quasi-stable state.

Then the thermal conductivity λ and the specific heat c of the sample can be calculated as:

$$c = \frac{q_c}{\rho R \frac{dt}{d\tau}} \tag{11}$$

$$\lambda = \frac{q_c R}{2\Delta t} \tag{12}$$

This model can be simulated on COMSOL as well.

2.2 Major instruments and materials

2.2.1 The resistor thermal model

Four resistors with different resistance values were connected in series and embedded in the sponge (Fig. 3a). Different currents were provided, and the thermocouples were placed in the centers of the surfaces of each resistor.

2.2.2 The plate thermal model

As illustrated in Fig. 3b, four samples of the same size were placed in a square grid with two heaters embed symmetrically within two adjacent samples on both sides, providing stable heat flux. Outside the sample there were insulator which exchanged heat with surroundings following the Newton's cooling law. Two themocouples were placed at the central face and the heating face of the model, respectively.

2.2.3 CompactDAQ multichannel data acquisition system and LabVIEW virtual instrument

A. CompactDAQ

In this research we use CompactDAQ platform ($NI\ CDAQ\ NI$ 9171) integrated with high density thermocouples module (NI 9211) to collect the temperature measurements data.

CompactDAQ is a data acquisition platform built by National Instruments that includes a broad set of compatible hardware and software. CompactDAQ integrates hardware for data I/O with LabVIEW software to enable researchers to collect, process, and analyze sensor data. It can be directly connected to various kinds of sensors and manage multichannel data c tasks simultaneously.

The high density thermocouple module (NI 9211) is a multichannel temperature measuring instrument that can link to up to four thermocouples (Fig. 4a and Fig. 4b). The data collected in each acquisition channel will be preprocessed and transformed into digital signals by a 24-bit ADC (Fig. 4c).

B. LabVIEW virtual instrument

Data collected from CompactDAQ platform can be directly imported and processed by the LabVIEW software. In this research, we programmed and built a virtual thermometer in the LabVIEW platform and used it to integrate the temperature measurements. The program and panel interface are illustrated in Fig. 5a and Fig. 5b, respectively.

2.2.4 Multiphysics simulation platform COMSOL

COMSOL Multiphysics is a cross-platform finite element analysis solver and multiphysics simulation software. It allows conventional physics-based user interfaces and coupled systems of partial differential equations. COMSOL provides an IDE and unified workflow for electrical, mechanical, fluid, acoustic, and chemical applications.

In this research, the thermal models of resistor and plate were built and simulated on COMSOL platform, and the distribution of the temperature fields and their evolution over time were obtained.

2.3 Method

For the resistor thermal model, different currents were provided to the series resistors and changes of surface temperature of every resistor over time were collected. After equilibrium was reached, the current was removed, and the cooling curves were obtained. The relationship between equilibrium temperature and heating power were also investigated.

For the thermal model of the plate, with continuous injection of stable heat into the system, after the system reached the quasi-stable stage, the temperature difference between the surface and the center face Δt and the rate of temperature changes in the center face $\frac{dt}{d\tau}$ were calculated.

For both models, the real-world experiments and COMSOL simulation experiments were conducted, and their results were compared.

3 Result

3.1 The resistor thermal model

A. Real-world experiment

Four resistors with different resistance values were connected in series and embedded in the sponge. With different currents provided, the heating curves and the following cooling curves (Fig. 6) were obtained from the thermocouples placed on each resistor. The results show that for the resistor heating model, as the current starts to flow through the resistor, the surface temperature began to increase. After a rapid climbing of the temperature, the thermal system gradually reached an equilibrium, and the temperature finally become stable. If the current was removed, the temperature began to drop and finally reached room temperature.

The equilibrium temperatures of each resistor were defined as the maximum temperature before the cooling process, and their correlation with the heating power is shown in Fig. 7. Results show that the equilibrium temperature was directly proportional to the resist value.

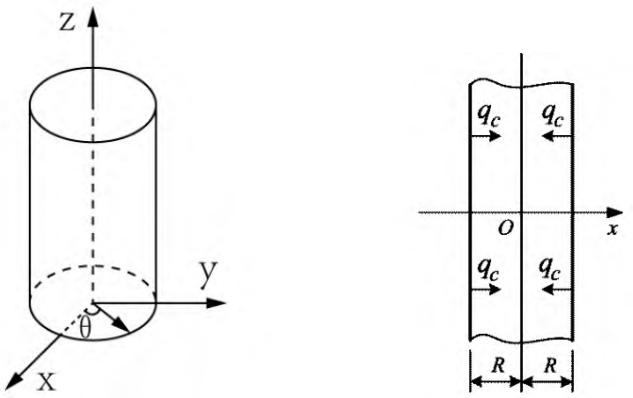

(a) The ideal resistor thermal model (b) The ideal plate thermal model

Figure 1: **Illustration of the two ideal thermal models**

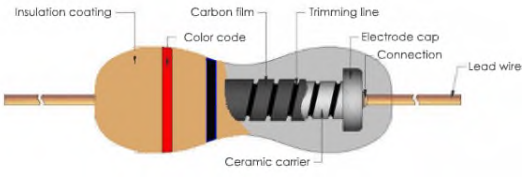

Figure 2: **The structure of a resistor**

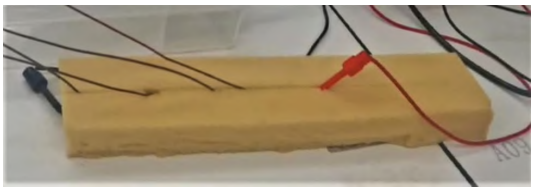

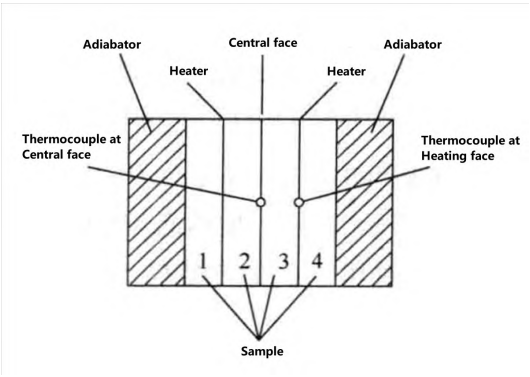

(a) The resistor thermal model (b) The plate thermal model

Figure 3: **Illustration of the two thermal models**

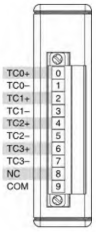

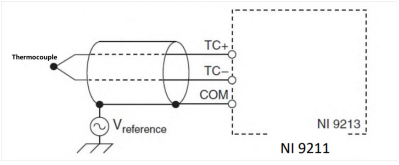

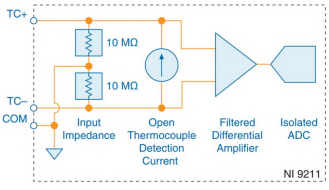

(a) Schematic of the pins (b) Schematic of connection (c) Schematic of the signal processing

Figure 4: **High density thermocouples module (*NI* 9211)**

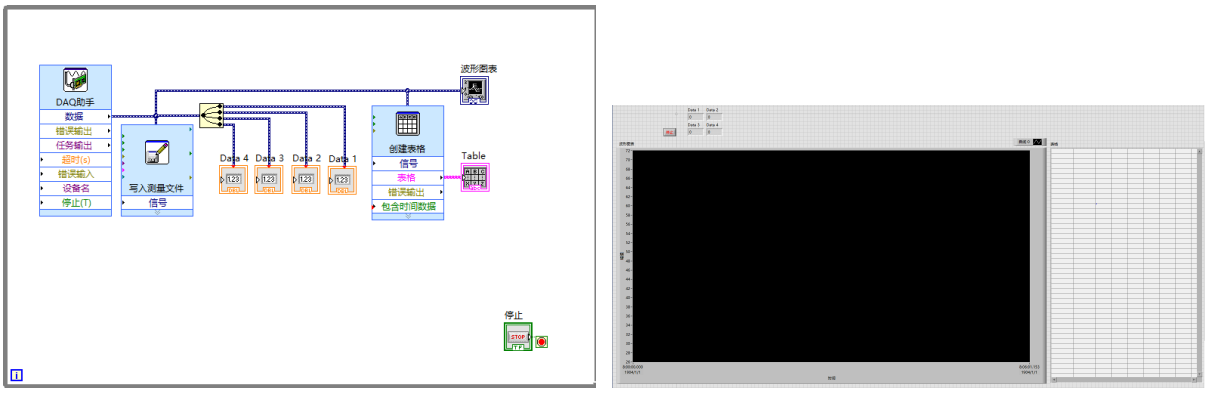

(a) The program interface (b) The panel interface

Figure 5: **Virtual thermometer**

Simultaneously, the simulation experiments were conducted.

B1. Simulation: The ideal model

To begin with, we first built the ideal resistor thermal model (As illustrated in Fig. 1a) and run the simulation on COMSOL platform. The geometric model of the ideal resistor thermal model is shown in Fig. 8. The top and bottom surfaces of the resistor were set as adiabatic, and the side faces were able to exchange heat with surroundings following the Newton's cooling law. With different currents provided, the heating curves were obtained(Fig. 9), and the correlation of the equilibrium temperatures of each resistor and the heating powers were shown in Fig. 10.

Results show that the equilibrium temperature was directly proportional to the resist value, which is consistent with the real-world experiment.

B2. Simulation: The complex model

Next, we built the complex resistor thermal model basing on the actual structure of the resistor(Fig. 2) and run the simulation on COMSOL platform. The geometric model of the thermal model of the complex resistor thermal model was shown in Fig. 11, in which the resistor, which was composed of a copper shell and a ceramic core, was linked in series and embedded in the sponge. With different currents provided, the heating curves and the following cooling curves were obtained(Fig. 12), and the correlation of the equilibrium temperatures of each resistor and the heating powers were shown in Fig. 13.

Results show that the equilibrium temperature was directly proportional to the resist value, which is consistent with the real-world experiment and the previous simulation model.

C. Comparison of the three models

The equilibrium temperature of each reistor obtained from the real-world experiment, simulation on the ideal model and simulation on the complex model are summarized in Tab. 1

Out of our expectation, we found that the ideal model was even more accurate than the complex mode. The heating time needed to reach the equilibrium and the final equilibrium temperature of the ideal model were all consistent with the real-world model, while for the complex model, there's a great difference. We hypothesize that as the complex model involved much more details, the accuracy of the values of material properties and geometric dimensions becomes more essential and may have a more prevalent influence on the results. Due to lack of these necessary knowledge, the parameters were all set empirically, which may cause the results to be inaccurate.

Anyway, the tendencies and general patterns of temperature changes are consistent among the three models, which proves the effectiveness of these techniques in studying thermal conducting models with very complex boundary conditions.

To further improve the performance of the model, accurate values of parameters involved in the model are required, and the geometric structure of the model is also required to improve.

3.2 The plate thermal model

A. Real-world experiment

As shown in Fig. 3b, four samples of the same size were placed in a square grid with two heaters symmetrically embedded within two adjacent samples in both sides, which provides stable heat flux. Outside the sample there were insulator which exchanged heat with surroundings following the Newton's cooling law. The two themocouples were placed at the central face and the heating face, respectively.

The change of temperature of the central face (Fig. 14a) and the temperature difference between the heating face and the central face (Fig. 14b) were obtained for samples made of rubber or organic glass. Results show that the for both materials, after a short period of non-linear increasing of the temperature, the system finally reached the quasi-stable state, in which the temperature was directly proportional to the heating time. At the same time, the temperature difference

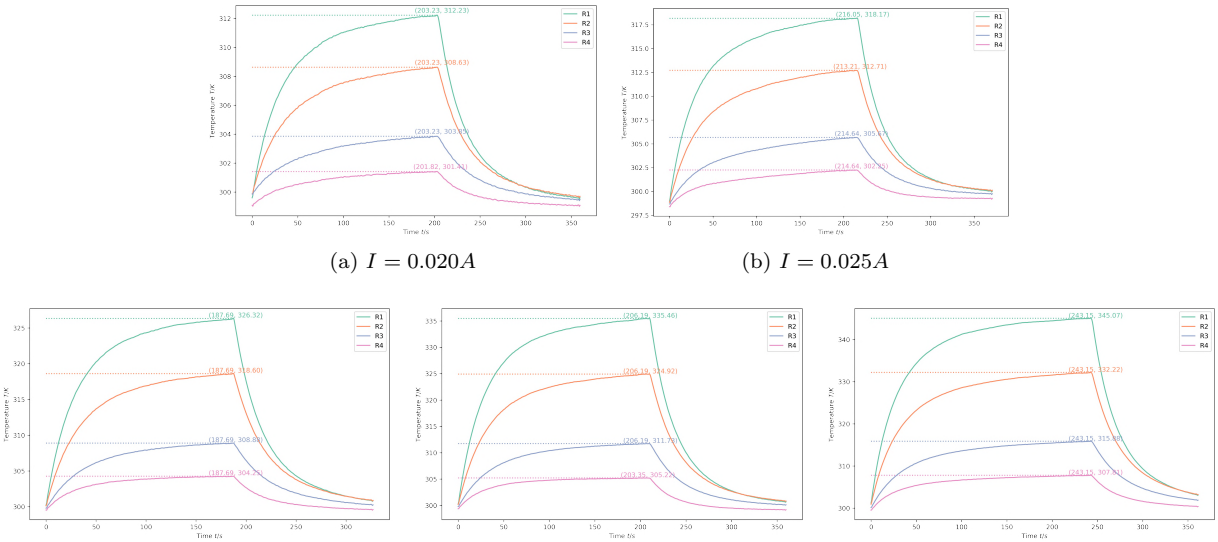

(a) $I = 0.020A$ (b) $I = 0.025A$

(c) $I = 0.030A$ (d) $I = 0.035A$ (e) $I = 0.040A$

Figure 6: **Heating and cooling curves of the series resistors under different currents, real-world experiments**

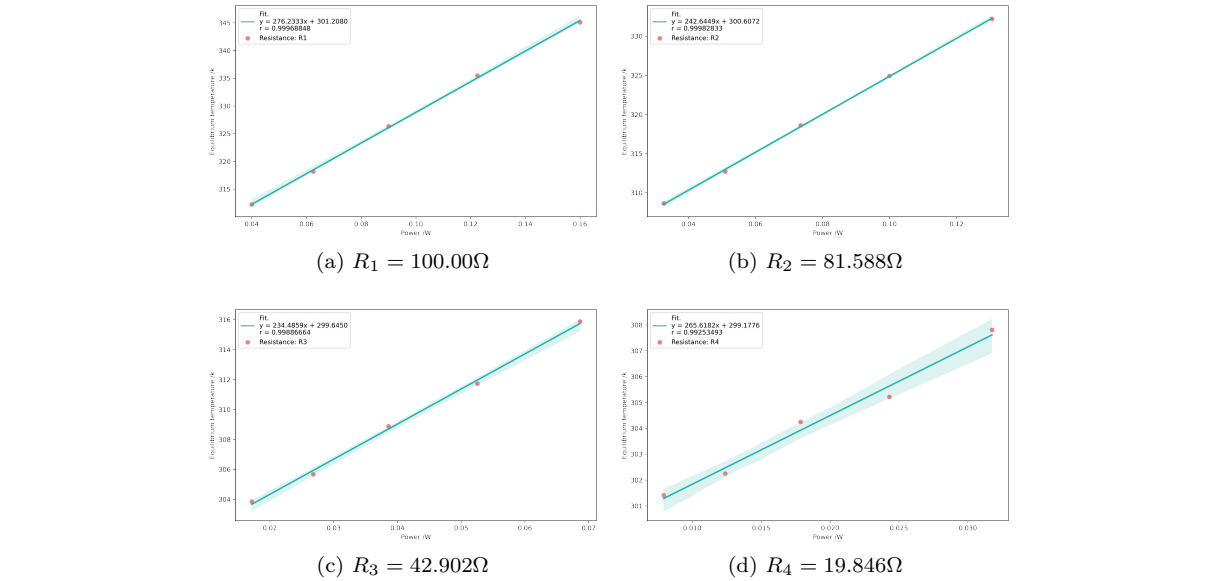

(a) $R_1 = 100.00\Omega$ (b) $R_2 = 81.588\Omega$

(c) $R_3 = 42.902\Omega$ (d) $R_4 = 19.846\Omega$

Figure 7: **Correlation of equilibrium temperature and the heating power, real-world experiments**

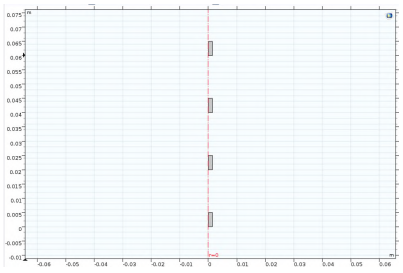

Figure 8: **The geometric model of the ideal resistor model**

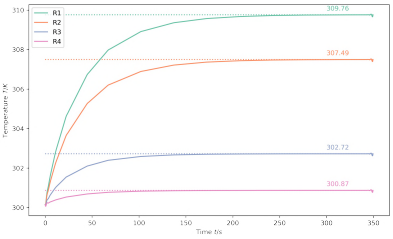

(a) $I = 0.020A$

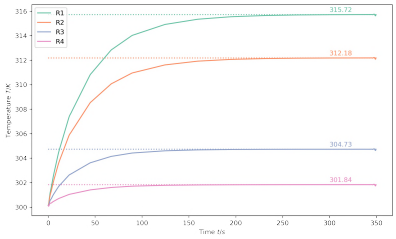

(b) $I = 0.025A$

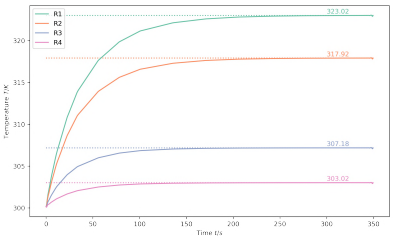

(c) $I = 0.030A$

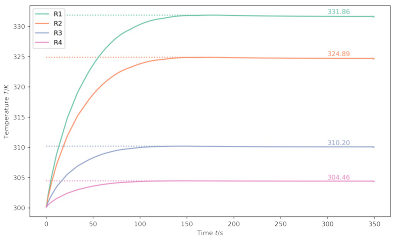

(d) $I = 0.035A$

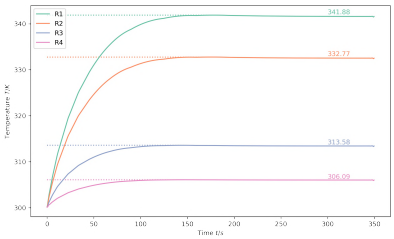

(e) $I = 0.040A$

Figure 9: **Heating curves of the series resistors under different currents, simulation experiments of the ideal model**

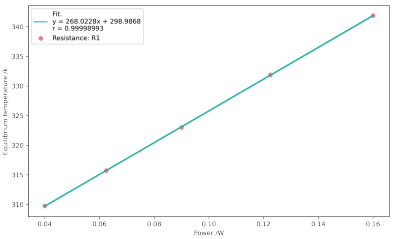

(a) $R_1 = 100.00\Omega$

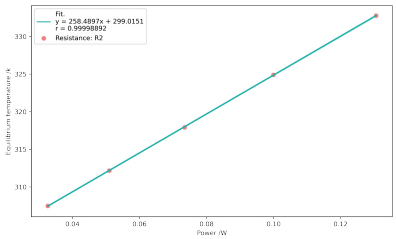

(b) $R_2 = 81.588\Omega$

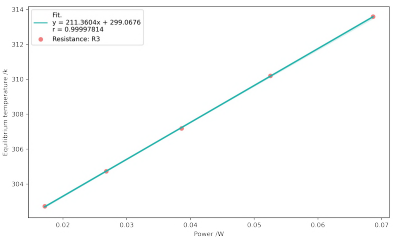

(c) $R_3 = 42.902\Omega$

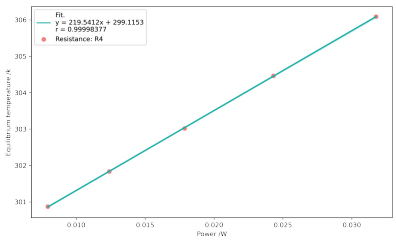

(d) $R_4 = 19.846\Omega$

Figure 10: **Correlation of equilibrium temperature and the heating power, simulation experiments of the ideal model**

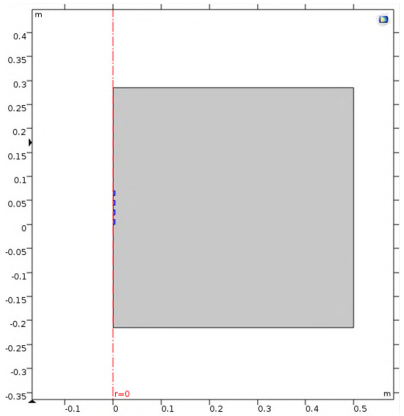

Figure 11: **The geometric model of the complex resistor model**

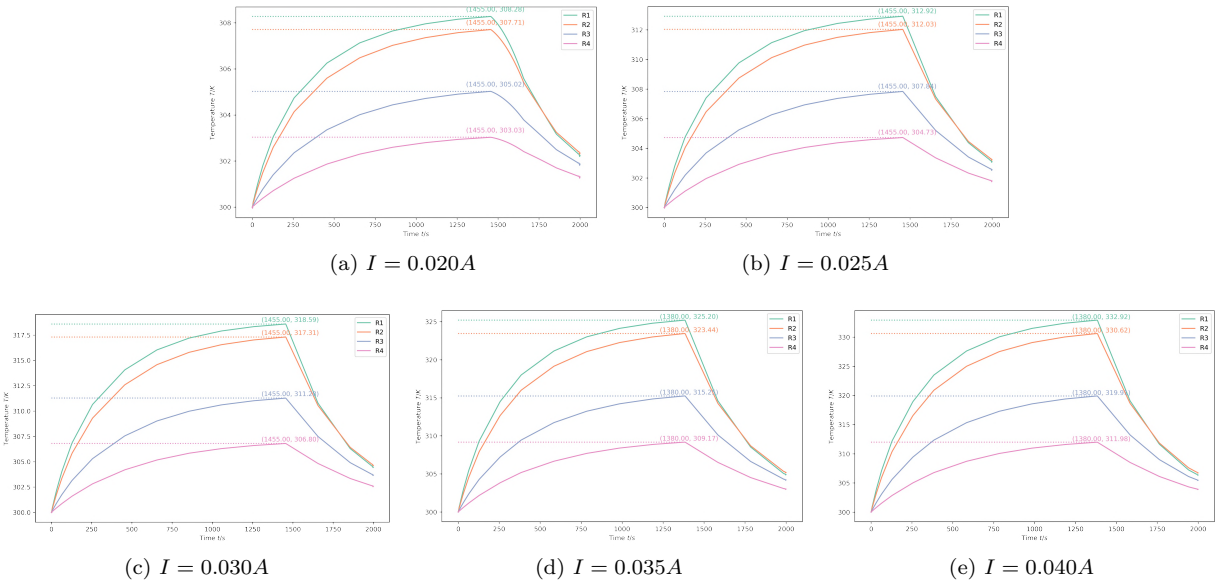

(a) $I = 0.020A$ (b) $I = 0.025A$

(c) $I = 0.030A$ (d) $I = 0.035A$ (e) $I = 0.040A$

Figure 12: **Heating and cooling curves of the series resistors under different currents, simulation experiments of the complex model**

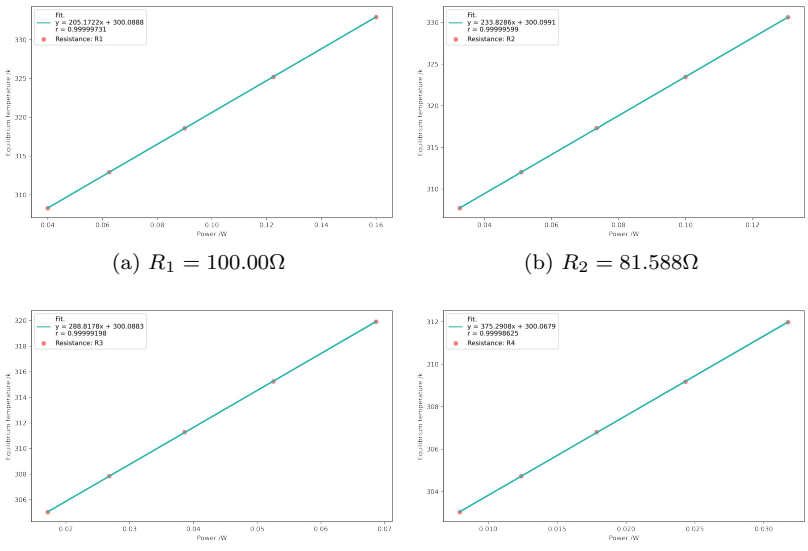

(a) $R_1 = 100.00\Omega$ (b) $R_2 = 81.588\Omega$

(c) $R_3 = 42.902\Omega$ (d) $R_4 = 19.846\Omega$

Figure 13: **Correlation of equilibrium temperature and the heating power, simulation experiments of the complex model**

Table 1: **Summary of the equilibrium temperatures of the resistors**

Current	Resistor	Real-world Mod.	Sim. Ideal Mod.	Sim. Complex Mod.
$0.020A$	R_1	312.23	309.76	308.28
	R_2	308.63	307.49	307.71
	R_3	303.85	302.72	305.02
	R_4	301.41	300.87	303.03
$0.025A$	R_1	318.17	315.72	312.92
	R_2	312.71	312.18	312.03
	R_3	305.67	304.73	307.84
	R_4	302.25	301.84	304.73
$0.030A$	R_1	326.32	323.02	318.59
	R_2	318.60	317.92	317.31
	R_3	308.88	307.18	311.28
	R_4	304.25	303.02	306.80
$0.035A$	R_1	335.46	331.86	325.20
	R_1	324.92	324.89	323.44
	R_1	311.73	310.20	315.25
	R_1	305.22	304.46	309.17
$0.040A$	R_1	345.07	341.88	332.92
	R_2	332.22	332.77	330.62
	R_3	315.88	313.58	319.92
	R_4	307.81	306.09	311.98

between the heating face and the central face also became stable.

The equilibrium temperature difference and the changing rate of the central-face temperature were calculated, which are summarized in the Tab. 2.

Simultaneously, the simulation experiments were conducted.

B1. Simulation: The ideal model

To begin with, we first built the ideal thermal model (As illustrated in Fig. 1b) and run the simulation on COMSOL platform. The geometric model of the ideal resistor thermal model is shown in Fig. 15. The surfaces of the model were allowed to exchange heat with surroundings following the Newton's cooling law. With stable current provided, the two membrane-like heaters continuously provided stable heat flux, and the temperature of the samples began to raise. The change of temperature of the central face (Fig. 16a) and the temperature difference between the heating face and the central face (Fig. 16b) were obtained for samples made of rubber or organic glass.

Results show that at the quasi-stable state, the temperature was directly proportional to the heating time and the temperature difference between the heating face and the central face was stable, which is consistent with the real-world experiment.

B2. Simulation: The complex model

Next, we built the complex plate thermal model in which the samples were embedded in the insulator and run the simulation on the COMSOL platform. The geometrical model of the complex thermal model is shown in Fig. 17. With stable current provided, the two membrane-like heaters continuously provided stable heat flux, and the temperature of the samples began to raise. The change of temperature of the central face (Fig. 18a) and the temperature difference between the heating face and the central face (Fig. 18b) were obtained for samples made of rubber or organic glass.

Results show that at the quasi-stable state, the temperature was directly proportional to the heating time and the temperature difference between the heating face and the central face was stable, which is consistent with the real-world experiment.

C. Comparison of the three models The equilibrium temperature different between the central face and heating face and the changing rate of temperature at the quasi-stable state obtained from the three experiments are summarized in Tab. 2.

Still, out of our expectation, we found that the ideal model was even more accurate than the complex mode. The final equilibrium temperature difference and the heating rate of the central face of the ideal model were all consistent with the real-world model, while for the complex model, there is a great difference. Basing on the same hypothesis, that is, lack of necessary knowledge of the materials and the geomagnetic diameters will induce great uncertainty to the model, we admit that further improvement of the model is required.

Anyway, the tendencies and general patterns of temperature changes are consistent among the three models, which proves the effectiveness of these techniques in studying thermal conducting models with very complex boundary conditions.

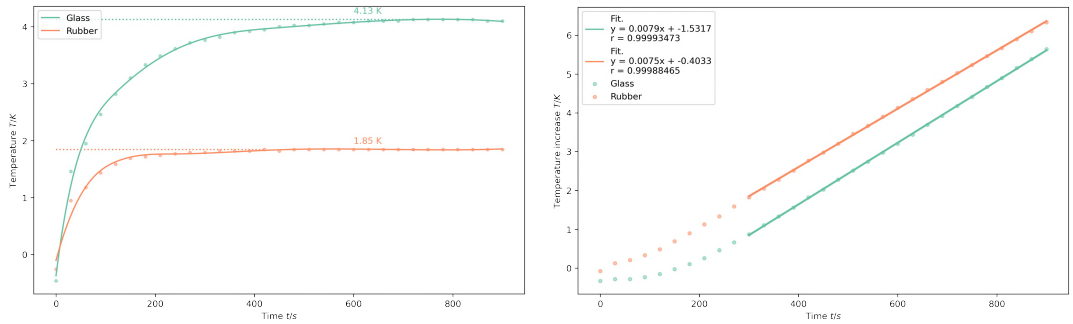

(a) Temperature of the central face (b) Temperature difference

Figure 14: **Thermal conduction of rubber or glass, real-world experiments**

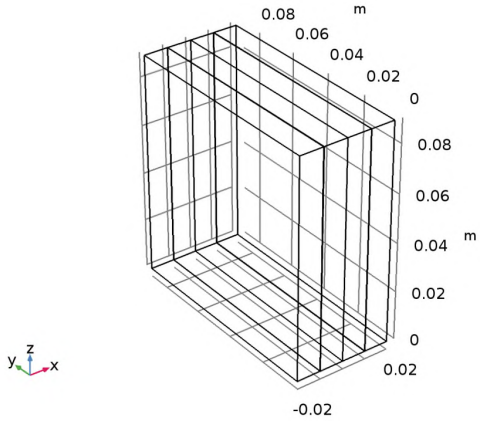

Figure 15: **The geometric model of the ideal plate model**

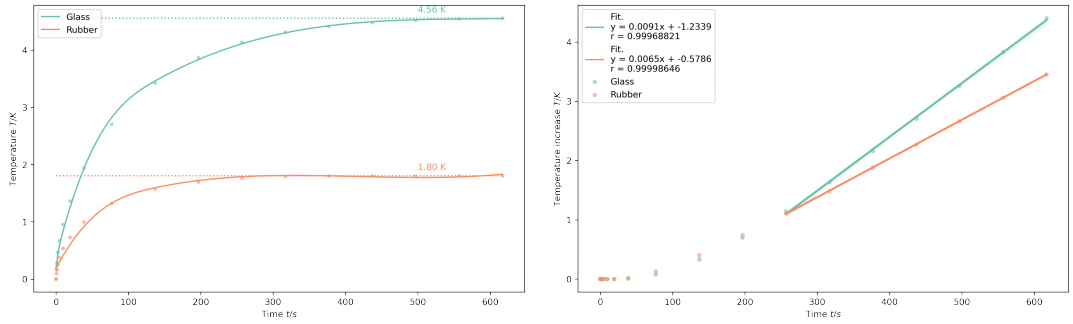

(a) Temperature of the central face (b) Temperature difference

Figure 16: **Thermal conduction of rubber or glass, simulation experiments of the ideal model**

Table 2: **Summary of the equilibrium temperature difference and heating rate**

Sample	Par.	Real-world EXP.	Sim. Ideal mod.	Sim. Complex Mod.
Organic glass	Heating rate (K/s)	0.0079	0.0091	0.0054
	Temperature difference (K)	4.13	4.56	5.25
Rubber	Heating rate (K/s)	0.0075	0.0065	0.0046
	Temperature difference (K)	1.85	1.80	2.13

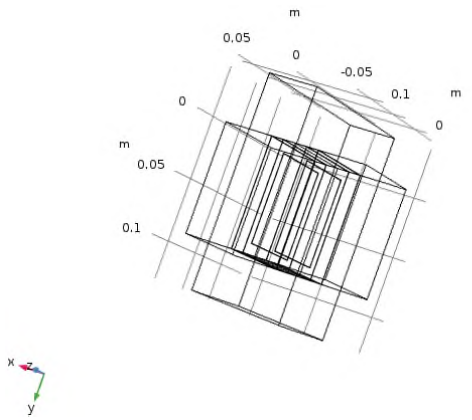

Figure 17: **The geometric model of the complex plate model**

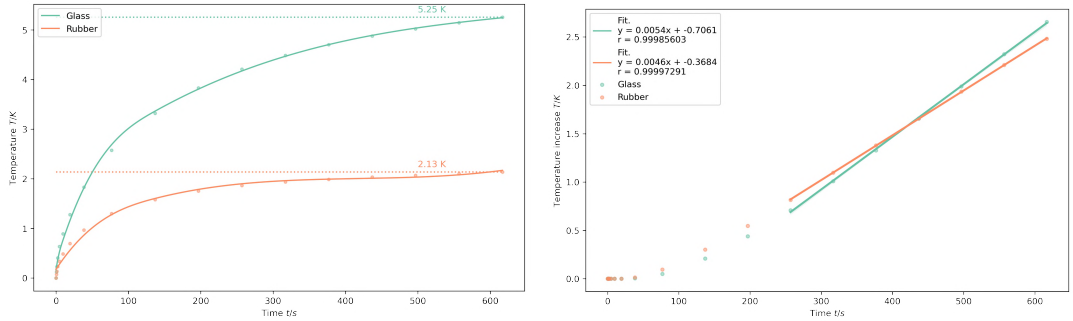

(a) Temperature of the central face

(b) Temperature difference

Figure 18: **Thermal conduction of rubber or glass, simulation experiments of the complex model**

4 Conclusion and Discussion

4.1 Conclusion

In conclusion, in this research we conducted real-world temperature measurement basing on LabVIEW platform, and simulation experiments basing on COMSOL for both the resistor thermal model and the plate thermal model, and revealed the characteristics of temperature fields of these models and their evolution over time. Although the measurement values obtained from real-world experiments and simulation experiments were not exactly consistent, the tendencies and general patterns of temperature changes are identical, which proves the effectiveness of these techniques in studying thermal conducting models with very complex boundary conditions.

4.2 Known limitation

As the complex model involved much more details, the precision of the values of the material properties and geometric dimensions becomes so essential that they have a dominant influence on the results. Due to lack of these necessary knowledge, however, the parameters were all set empirically in this research, which definitely will cause the results to be inaccurate.

To further improve the performance of the model, it is critical to ascertain the accurate value of parameters involved in the model.

Reference

1. H. Shen, *General Physics Laboratory* (Science press, 2015), ISBN: 978-7-03-043311-4 (cit. on p. 2).

C8 Revealing temperature fields of thermal models basing on multichannel measurement and simulation

SUPPLEMENTARY INFORMATION

Experimenter: Zweig, Wong 20980066
Participant: Runbing Mo 20980131
Date: 2022-05

Contents

1 Materials and instruments

Table S1: **Materials and instruments**

Name	Total	Model and parameters
CompactDAQ	1	$NI\ CDAQ\ NI-9171$
Thermocouple acquisition module	1	$NI\ 9211$
Resistance	4	$100.000\Omega, 81.588\Omega, 42.902\Omega, 19.846\Omega$
COMSOL	1	6.0

2 Exp.1 Resistor model

2.1 Main parameters

The resistance value and currents provided are summarized in Tab. S2. The values of properties of different materials adapted in the simulation experiment are summarized in Tab. S3.

$C_p(J/kg\cdot K)$: Specific heat capacity at constant pressure; $\rho(kg/m^3)$: Density; $k(W/m\cdot K)$: Thermal conductivity.

Table S2: **Resistors and currents**

Item	parameters
R_1	100.000Ω
R_2	81.588Ω
R_3	42.902Ω
R_4	19.846Ω
I_1	$0.020A$
I_2	$0.025A$
I_3	$0.030A$
I_4	$0.035A$
I_5	$0.040A$

Table S3: **Material properties**

Material	$C_p(J/kg\cdot K)$	$\rho(kg/m^3)$	$k(W/m\cdot K)$
Copper(Heater)	385	8700	400
Silicon(Core)	700	2329	130
Sponge(Insulator)	1	1700	0.09

2.2 Supplementary data and figure

1. Fig. S1: Temperature field distribution of the ideal resistor model.
2. Fig. S2: Temperature field distribution of the complex resistor model.

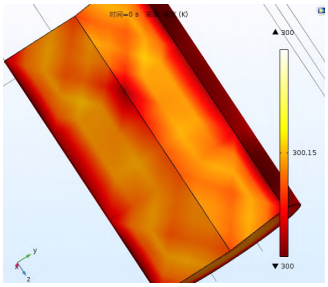

(a) $I = 0.020A$

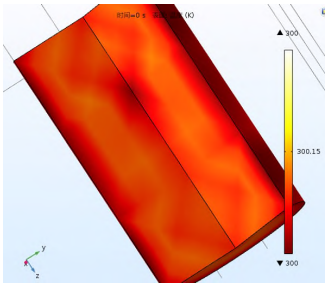

(b) $I = 0.025A$

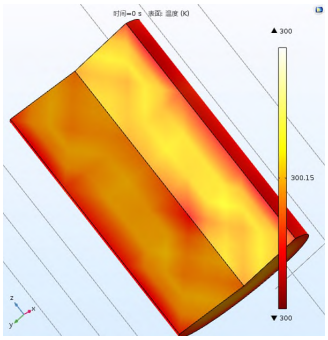

(c) $I = 0.030A$

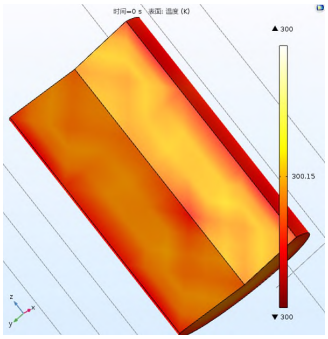

(d) $I = 0.035A$

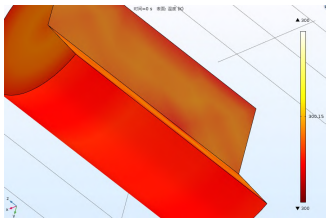

(e) $I = 0.040A$

Figure S1: **Temperature field distribution of the ideal resistor model.**

2.3 Question

2.3.1 What are Dirichlet condition, Neumann condition and Robin condition? Which of them can COMSOL deal with?

1. Dirichlet condition: The temperature of the boundary is fixed ($u_{|s} = u_0(r,t)$).
2. Neumann condition: The temperature of the boundary is determined by the heat flux ($\frac{\partial u}{\partial n}_{|s} = \frac{q(r,t)}{k}$).
3. Robin condition: The temperature of the boundary is determined by Newton's cooling law ($(\frac{\partial u}{\partial n} + hu)_{|s} = hu_0(r,t)$).
4. COMSOL is capable of dealing with all three types of conditions.

2.3.2 Improve the performance of the model

1. Refine the structure of the model: For instance, the model of the resistor can be further refined by adding the electrodes and the insulating layer and so on.

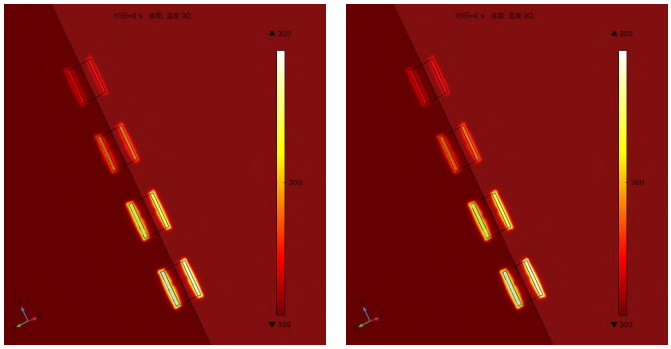

(a) $I = 0.020A$ (b) $I = 0.025A$

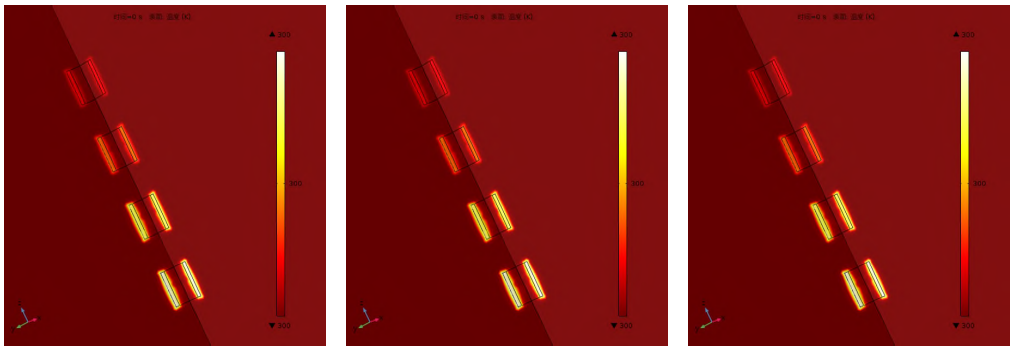

(c) $I = 0.030A$ (d) $I = 0.035A$ (e) $I = 0.040A$

Figure S2: **Temperature field distribution of the complex resistor model.**

2. Ascertain the accurate values of the properties of materials: Accurate values of the properties of materials should be carefully measured in real-world experiments rather than using empirical values.

3. Increase the complexity of computation: A finer mesh and greater number of sampling points, if available, may increase the accuracy of the model.

3 Exp.2 Plate model

3.1 Main parameters

Parameters including the resistance value of the heater($r/Omega$), the heating voltage(U/V), default Area correction factor(A), and the heat exchange coefficient(H) are shown in Tab. S4. Values of properties of different materials adapted in the simulation experiment are summarized in Tab. S5. $C_p(J/kg \cdot K)$: Specific heat capacity at constant pressure; $\rho(kg/m^3)$: Density; $k(W/m \cdot K)$: Thermal conductivity.

3.2 Supplementary data and figure

1. Fig. S3: Temperature field distribution of the four models.

2. Fig. S4: Change the area correction factor A for Model 1.

Table S4: **Parameters**

Item	parameters
Heating voltage U	$17.0V$
Resistance R	$110/Omega$
Area correction factor$A$	0.85
Heat exchange coefficient$H$	50

Table S5: **Material properties**

Material	$C_p(J/kg \cdot K)$	$\rho(kg/m^3)$	$k(W/m \cdot K)$
Organic glass(Sample)	1333	1196	0.168
Rubber(Sample)	1700	1374	0.426
Aluminum(Heater)	972.5	2676.8	67.09
Film(Heater)	1058	1533	33.97
Frame(Insulator)	920	1900	0.90
Sponge(Insulator)	400	4200	0.046

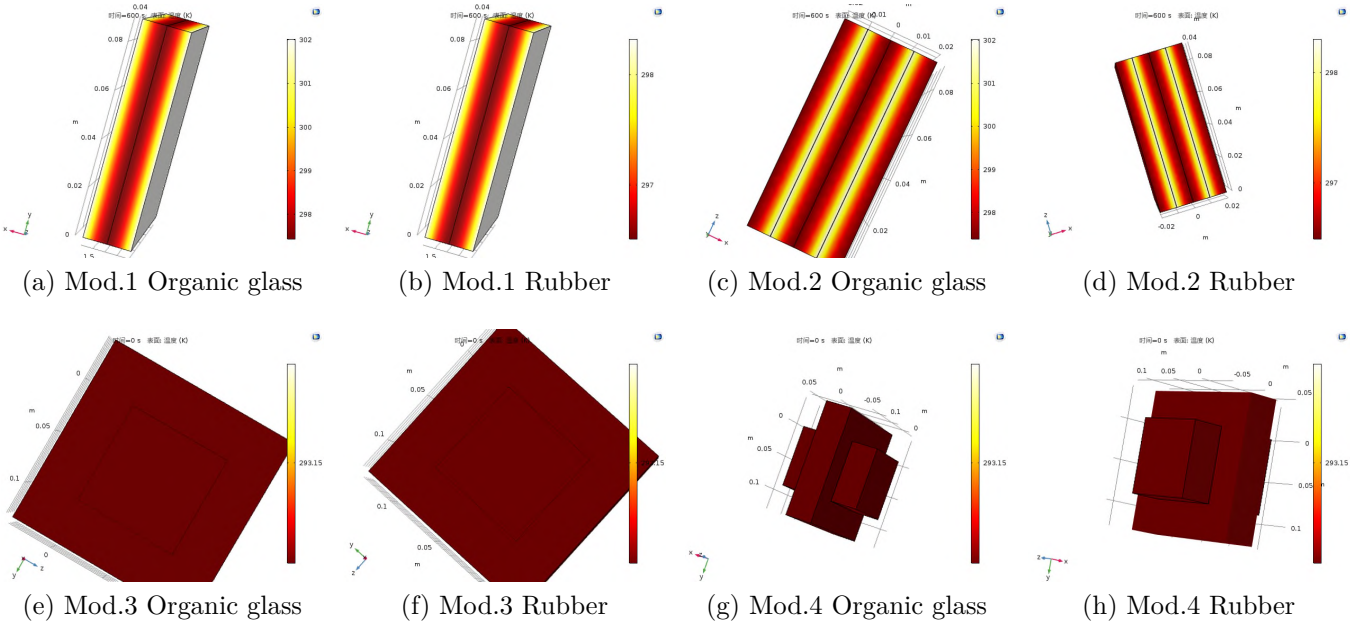

(a) Mod.1 Organic glass (b) Mod.1 Rubber (c) Mod.2 Organic glass (d) Mod.2 Rubber

(e) Mod.3 Organic glass (f) Mod.3 Rubber (g) Mod.4 Organic glass (h) Mod.4 Rubber

Figure S3: **Temperature field distribution of the ideal resistor model.**

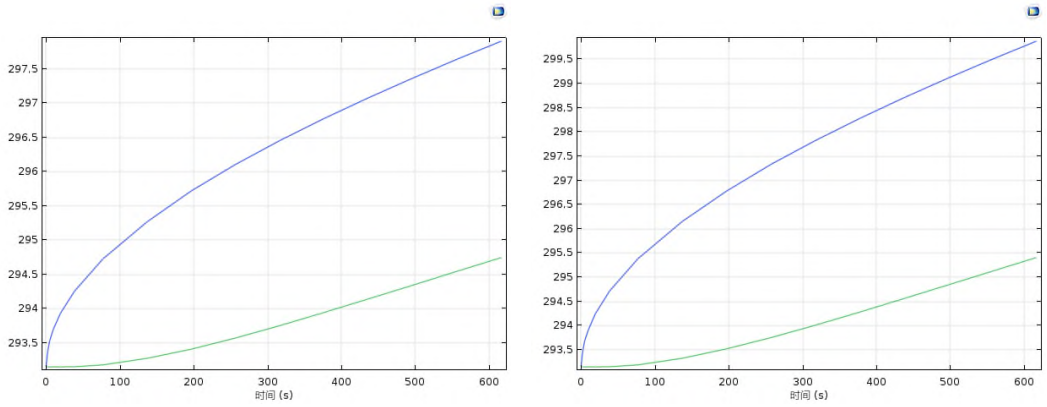

(a) Mod.1 $A = 0.60$ (b) Mod.1 $A = 0.85$

Figure S4: **Change the area correction factor A for Model 1**

3.3 Question

3.3.1 Why to set the area correction factor A?

The area correction factor is used to correct the area of the heater to eliminate the edge effect. In the four-sample model, the heat flux $\boldsymbol{q}$ can be expressed as:

$$\boldsymbol{q} = \frac{U^2}{2Fr} \tag{1}$$

where $F = AS$ is the heating area after correction of the edge effect, A is the area correction factor, and S is the actual area of the heater.

$\boldsymbol{A}$ sometimes need to be adjusted empirically as illustrated in Fig. S4. We found that if the area correction factor is set to 0.6, the results are more approximate to the results of real-world experiment.

4 Data and code availability

Data and code are available at https://github.com/Jeg-Vet/SYSU-PHY-EXP/tree/main/